International Journal of Engineering Research & Technology (IJERT)
ISSN: 2278-0181
Vol. 15 Issue 06 , June - 2026

Design and Structural Analysis of an Electric Tricycle using Double Wishbone Suspension.

Vivek Gurav[1], Preetam Selmokar[2], Nagesh Chougule[2,] Chinmay Desai[2]
[12]Department of Mechanical Engineering, COEP Technological University, Pune, India.

Abstract: Rapid growth in urban mobility demands energy efficient, compact, and economical transportation solutions. This paper presents the design and structural analysis of an electric tricycle that bridges the gap between conventional two wheelers and four-wheelers, combining maneuverability with improved stability and efficiency. The objective is to develop a vehicle using appropriate subsystems that ensure improved ride comfort and handling performance. A complete model, including the chassis, double wishbone suspension, hub, knuckle, and EV transmission system, was developed for this purpose.

CAD models were created using ANSYS Spaceclaim, and static and fatigue analyses were carried out using ANSYS Workbench under realistic and worst-case loading conditions, including vertical, braking, and lateral loads. Materials such as AISI 4130, Mild Steel, and aluminum alloys (6061-T6, 7075-T6) were evaluated for strength, weight, fatigue life, and cost. The results confirm the structural integrity of each component and demonstrate effective material optimization: AISI 4130 was selected for the wishbone and chassis for its superior fatigue performance and safety margin, while 6061-T6 was selected for the hub and knuckle, offering sufficient strength at lower weight and cost. Fatigue life across the components ranged up to 10^7 cycles under acceptable load cases, with stress levels and safety factors remaining within design limits across the operating range considered. The proposed electric tricycle's powertrain was designed to achieve a target speed of 40 to 50 km/h with suitable torque output from an electric motor and differential setup.

This paper shows that a well-engineered electric tricycle can serve as a sustainable mobility solution, offering reduced emissions, lower operating costs, and improved stability compared to conventional two-wheelers.

Keywords: *Double Wishbone, Knuckle, Hub, AISI 4130, Aluminum alloys (6061-T6, 7075-T6)*

1 INTRODUCTION

Growing urbanization and rising vehicle numbers have intensified the need for cleaner, more efficient transportation in India. Internal combustion engine (ICE) vehicles remain a primary source of greenhouse gas emissions and urban air pollution, making electric vehicles (EVs) a compelling alternative for greener mobility.

India's EV sector is expanding rapidly, with total sales reaching around 2.3 million units in 2025 and EV penetration at roughly 8% of all new vehicle registrations. Policy frameworks such as the FAME scheme and the PM E-DRIVE initiative have been instrumental in accelerating this shift away from fossil fuel dependence. Within the EV landscape, electric three-wheelers have achieved the strongest market uptake of any segment. They account for around 35% of India's total EV sales, and over 57% of all three-wheelers sold in the country are now electric. A transition rate higher than any other vehicle category. India is also the global leader in this segment, commanding more than half of worldwide electric three-wheeler sales.

Electric tricycles occupy a practical middle ground between two-wheelers and four-wheelers: more stable and load-capable than the former, yet more space-efficient. This makes particularly well suited for dense city environments and short-distance travel. Beyond congestion benefits and eliminate tailpipe emissions, reduce noise, and perform efficiently in stop-and-go traffic where electric drivetrains inherently excel.

Ride quality and handling in such vehicles are critically influenced by the suspension system. The double wishbone configuration is favored for its precise wheel control, favorable camber characteristics, and superior cornering stability. It also allows fine-tuned management of key suspension geometry parameters such as caster, camber, kingpin inclination, and roll center height. All of which directly shape dynamic behavior.

This project presents the design and structural evaluation of an electric tricycle incorporating a double wishbone suspension. Suspension hardpoints were derived using Lotus Shark software, and component models: chassis,

International Journal of Engineering Research & Technology (IJERT)
ISSN: 2278-0181
Vol. 15 Issue 06 , June - 2026

wishbone, hub, and knuckle were developed in ANSYS Spaceclaim. ANSYS Workbench was then used to perform static and fatigue analyses under vertical, braking, and lateral load conditions. Four materials were assessed: Mild Steel, AISI 4130, Aluminum 6061-T6, and Aluminum 7075-T6, with comparisons drawn across stress, deformation, fatigue life, and safety margins to identify the optimal design material for each component.

2 LITERATURE REVIEW AND OBJECTIVES

The rapid growth of electric mobility in India has increased the demand for lightweight, energy-efficient, and structurally reliable vehicle platforms, particularly for low-cost urban transportation applications [7]. Government initiatives such as the FAME scheme and the PM E-DRIVE program have further encouraged the development of electric three-wheelers and other sustainable mobility solutions [8]. As a result, research on electric vehicle chassis, suspension systems, and wheel assemblies has gained significant importance.

Vehicle dynamics and stability are strongly influenced by suspension geometry and load transfer characteristics. Milliken and Milliken highlighted that suspension design directly affects handling, cornering stability, tire contact, and overall dynamic behavior of a vehicle [1]. Similarly, Gillespie established the fundamental relationship between suspension kinematics, weight transfer, braking performance, and vehicle stability, making these principles essential for the design of lightweight electric vehicles [3]. These studies provide the theoretical basis for selecting an independent suspension configuration for improved ride and handling characteristics.

Recent research has focused on the structural analysis of suspension systems for electric vehicles. Patil et al. investigated a suspension system for a light electric vehicle using finite element analysis and demonstrated that optimized suspension geometry can effectively withstand braking, cornering, and vertical loading conditions while reducing structural weight [2]. Their work emphasizes the importance of FEA-based validation during the design stage of electric vehicle suspension components.

The wheel hub is another critical component responsible for transmitting radial, axial, and braking loads from the wheel to the suspension assembly. Shinde, Patil, and Jadhav performed a structural analysis of a wheel hub using finite element methods and concluded that stress distribution and deformation characteristics must be carefully evaluated to ensure durability under operating loads [4]. Their findings support the use of numerical analysis for validating hub strength and stiffness in lightweight vehicle applications.

Steering knuckle design has also been extensively studied in Formula SAE and all-terrain vehicle applications. Garde, Shinde, and Jirage presented the design and optimization of a hub and knuckle assembly for a Formula SAE car, demonstrating that material selection and geometric optimization can significantly reduce component weight while maintaining adequate structural strength [5]. Dusane et al. further analyzed steering knuckles for all-terrain vehicles under combined loading conditions and reported that finite element analysis is effective in identifying stress concentrations and improving fatigue performance [6]. These studies indicate that integrated analysis of the hub and knuckle is essential for achieving a reliable wheel assembly.

For the development of vehicle structural components, appropriate numerical modeling techniques are equally important. The ANSYS Workbench Mechanical User's Guide provides standard procedures for meshing, including automatic and patch-conforming tetrahedral meshing as well as beam element modeling for space-frame structures [9]. These meshing methods are widely adopted in automotive finite element analysis to improve solution accuracy while maintaining reasonable computational efficiency.

In addition to numerical analysis, the mechanical design of suspension members, mounting brackets, and load-bearing components requires consideration of standard machine design principles. Bhandari discussed the design methodology for machine elements subjected to static and fluctuating loads, including stress analysis, factor of safety selection, and material strength considerations [10]. These principles are applicable to the design of suspension arms, hub mounts, and chassis joints used in electric vehicle structures.

Although substantial literature exists on suspension, hub, and steering knuckle analysis for Formula SAE and all-terrain vehicles, most reported studies focus on four-wheeled vehicle configurations [2], [5], [6]. Limited research has been conducted on electric tricycles employing an independent rear double wishbone suspension integrated with a lightweight space-frame chassis. Conventional three-wheelers generally utilize trailing arm or rigid axle arrangements, which provide limited camber control and lateral stability during cornering. Therefore, a research

International Journal of Engineering Research & Technology (IJERT)
ISSN: 2278-0181
Vol. 15 Issue 06 , June - 2026

gap exists in the structural and dynamic evaluation of a rear double wishbone suspension system for electric tricycle applications.

The present work addresses this gap by designing and structurally analyzing an electric tricycle equipped with a front telescopic suspension and an independent rear double wishbone suspension. Finite element analysis is performed on the chassis, suspension components, steering knuckle, and wheel hub to evaluate stress distribution, deformation, and structural reliability under representative loading conditions.

The objectives of the present study are outlined as follows:

1. To design a compact electric tricycle with a front telescopic suspension and a rear double wishbone suspension for improved urban mobility.
2. To develop and validate the rear suspension geometry through kinematic analysis.
3. To model the chassis, suspension, steering knuckle, and wheel hub using CAD software.
4. To perform finite element analysis (FEA) for structural optimization by evaluating stress, deformation, factor of safety, and fatigue life.

3 MATERIAL SELECTION AND METHODOLOGY

3.1 Overall Design Approach

This study follows a structured, top-down design process for the electric tricycle. The work begins with the vehicle's basic specifications: mass, target speed, and operating conditions which form the basis for all subsequent calculations. From these specifications, suspension geometry and key hardpoints are established, followed by detailed CAD modeling of the chassis, wishbone, hub, and knuckle. Loads expected during real-world operation, including vertical, lateral, braking, and torque inputs, are then derived analytically and applied to each component through finite element analysis. The resulting stress, deformation, and fatigue behavior are evaluated against standard safety criteria to identify the most suitable material and configuration for each part, ensuring that the final design meets structural requirements while remaining lightweight and cost-effective.

3.2 Vehicle Specifications

These specifications set the foundation for this thesis — the suspension geometry, FEA boundary conditions, and powertrain sizing were all worked out using these base numbers.

- Gross vehicle weight: 300 kg, Weight Distribution: 40: 60 (Front: Rear)
- Maximum Speed: 50 k/h= 13.89 m/s, Road Gradient: 7°, Rear Tyres = 90/90-12

3.3 Suspension Geometry Design (Lotus Shark)

The double wishbone suspension geometry was developed in Lotus Shark by defining suspension type, wheelbase, track width, total weight, and dynamic parameters such as camber, caster, and roll-center behavior under bump and roll. The simulation generates a hardpoint coordinate system, which was used as the basis for designing the chassis, wishbone, knuckle, and hub.

Track width was set at 750 mm (a 50 mm increase for improved packaging), with a ground clearance of 135 mm and CG height of 250 mm. Static camber and toe were set to 0°. Through ±3° of roll, camber varied from −1.9° to +1.5°; under bump travel of −20 mm to +40 mm, camber ranged from +1.1867° to −3.5497°, with spring travel of +11.91 mm (rebound) to −22.87 mm (bump). The geometry was optimized to maintain a favorable roll-center location across bump and roll conditions while meeting wheel-assembly packaging constraints.

The finalized hardpoints were exported to and used to build a wireframe reference layout, ensuring accurate alignment of the suspension, steering, and structural members for the chassis, wishbone, hub, and knuckle design that followed. Fig.1 shows bump condition and Fig.2 shows rolling condition

International Journal of Engineering Research & Technology (IJERT)
ISSN: 2278-0181
Vol. 15 Issue 06 , June - 2026

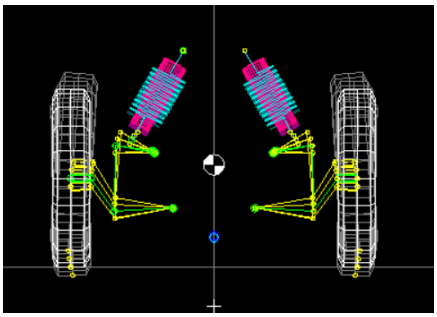

Fig.1 Bump Condition

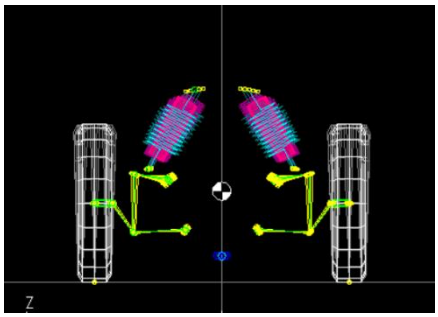

Fig.2 Roll Condition

3.4 CAD Modeling (ANSYS Spaceclaim)

The hardpoints from Lotus Shark were imported into ANSYS Spaceclaim to model the chassis, wishbone, hub, and knuckle, keeping mounting points and joint locations consistent with the suspension kinematics. The chassis was built as a tubular space frame using 25 × 1 mm tube for main members and 20 × 1.65 mm for supporting members, laid out around the suspension hardpoints, battery, and payload area. The wishbone was modeled with two candidate cross-sections, 18 × 1.65 mm and 22 × 1.6 mm, with joint ends placed per the exported hardpoints. Since the rear axle is driven and does not steer, the knuckle and hub were modeled without steering provision. The knuckle connects the hub to the wishbones, supports the bearing and brake disc, carries drive torque to the wheel, and links to the chassis via a toe-link that controls toe angle through suspension travel rather than steering. Each part was modeled individually, then assembled and checked for interference across suspension travel before being exported to ANSYS Workbench for analysis.Fig.3 shows CAD model of hub and Fig.4 shows CAD model of Knuckle.

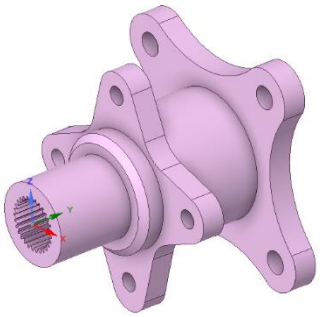

Fig.3 Hub

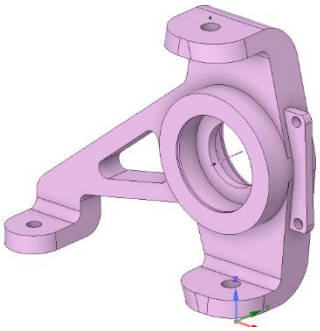

Fig.4 Knuckle

3.5 Load Calculation methodology:

Loads on the wishbone, hub, knuckle, and chassis were calculated analytically from the vehicle's mass, speed, and gradient specifications, forming the boundary conditions used in the FEA.

- **Vertical load**: derived from gross vehicle weight and rear-axle share (60%), with a 3g factor applied for worst-case bump loading alongside the baseline 1g case.
- **Drive torque**: calculated from total tractive force (gradient resistance + rolling resistance + aerodynamic drag at target speed), converted to wheel torque using wheel radius, and scaled by a design factor for FEA.
- **Lateral load**: calculated from cornering acceleration under normal (0.4g) and severe (0.6g) cornering cases.
- **Braking load**: derived from a 0.5g deceleration event, calculated two ways — as a direct force at the wishbone's ball joint, and as a torque-converted force at the hub's caliper mount, since these represent two points on the same braking load path.

International Journal of Engineering Research & Technology (IJERT)
ISSN: 2278-0181
Vol. 15 Issue 06 , June - 2026

3.6 Material Selection Criteria

Four materials were considered, each for a different reason. Mild Steel served as the baseline — cheap and easy to weld, but limited by its lower 250 MPa yield strength. AISI 4130 offered nearly double that strength at 460 MPa, at higher cost and machining difficulty, making it suited for high-load tubing applications. For the hub and knuckle, two aluminum grades were tested to cut rotating mass: 6061-T6 (276 MPa, easy to machine, inexpensive) and 7075-T6 (503 MPa, stronger but costlier and harder to work with).

Based on the FEA results, AISI 4130 was selected for the wishbone and chassis, since Mild Steel's safety factor fell below or close to 1.0 under harsher load cases. For the hub and knuckle, 6061-T6 was selected over 7075-T6, as it already cleared every load case with a comfortable margin, making the added strength and cost of 7075-T6 unnecessary. Table.1 shows material selection criteria.

Material	6061	7075	AISI	Mild
Strength	3	5	2	5
Machinability	5	2	5	4
Weldability	5	2	5	4
Cost	3	5	5	3
Availability	5	3	5	4

Table. 1

3.7 Finite Element Analysis Setup

All simulations were run in ANSYS Student Workbench using CAD geometry from ANSYS Spaceclaim. The wishbone, hub, and knuckle were meshed with 10-node tetrahedral (Tet10) elements via ANSYS's Automatic method, with local sizing at fillets, bores, and joints for accuracy in high-stress zones. Mesh independence study was conducted

. The chassis, a tubular space frame, was modeled as a line-body and meshed with beam elements along the tube centerlines — standard practice for frames and more efficient than meshing full tube geometry.

Boundary conditions matched each component's actual mounting and load path. For the wishbone, remote displacement was applied at the chassis-side mounts, with vertical, lateral, and braking forces at the ball joint — individually for 1g and 3g, together for combined loading. For the hub, the bearing seat was fixed, with vertical load for 1g/3g, and cornering force plus drive torque added for the combined and braking cases. For the knuckle, remote displacement was applied at its wishbone and toe-link connections, with hub-side loads carried through for each case. For the chassis, remote displacement was applied at the suspension mounts, with 1g, 3g, torsional, and side-impact loads applied as remote forces for their respective cases. Fig.5 and Fig.6 shows meshing used for wishbone and hub.

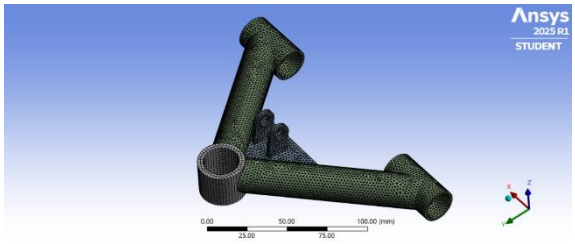

Fig.5 Wishbone Meshing

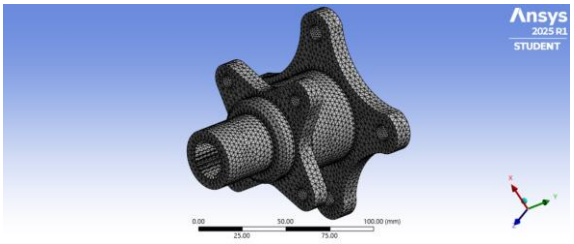

Fig.6 Hub Meshing

3.8 Evaluation Criteria

Two criteria decided pass/fail: factor of safety (FOS) and a fatigue-based safety factor, applied consistently across all four components. FOS was matched to load severity: 1.0–1.5 for steady loads, 2–3 for harsher cases like the 3g bump or side impact. Fatigue life targets depended on material: 10^7 cycles for steels (Mild Steel, AISI 4130), since they show a flattening S-N curve and 10^6 cycles for aluminum (6061-T6, 7075-T6), which has no true

International Journal of Engineering Research & Technology (IJERT)
ISSN: 2278-0181
Vol. 15 Issue 06 , June - 2026

endurance limit. A result passed only if it met both the FOS and fatigue targets for that load case; falling short on either, especially under harsher loads, resulting that material-section combination as inadequate.

4 Results

4.1 Wishbone Analysis

The wishbone links the wheel hub to the chassis, absorbing bump, cornering, and braking loads together. A finite element study in ANSYS Workbench checked stress, deformation, fatigue life, factor of safety, and fatigue-based safety factor for each load case. Fig.8 shows max stress at 3g loading and Fig.8 show deformation at 3g loading.

- **Static 1g:** Stress ~146.5 MPa, deformation ~0.10 mm for both materials. Mild Steel: FOS 1.71, fatigue safety factor 0.82 (660,070 cycles). AISI 4130: FOS 3.14, full 10^7 cycles (safety factor 1.37).
- **Static 3g:** Stress ~439 MPa (18×1.65 mm) / ~372 MPa (22×1.6 mm). Mild Steel: FOS 0.57–0.67 (fails), zero fatigue life. AISI 4130: FOS 1.05–1.34, 16,237–172,670 cycles.
- **Combined Loading:** Stress 170–174 MPa, deformation 0.047–0.054 mm. Mild Steel: FOS 1.46–1.47, safety factor 1.04–1.10. AISI 4130: FOS 2.64–2.68, safety factor 1.69–1.71, both at full 10^7 cycles.

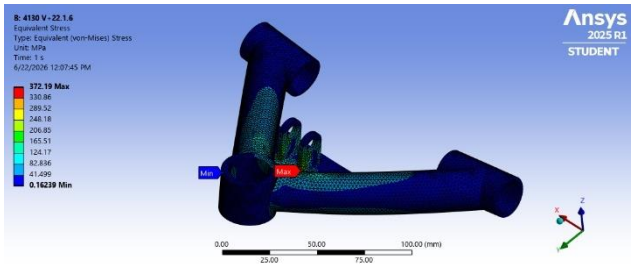

Fig.7 Stress at 3g Loading

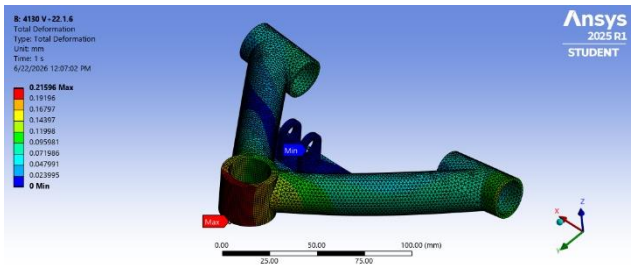

Fig.8 Deformation at 3g loading

4.2 Hub analysis

The wheel hub carries the wheel's full load while also passing through driving and braking torque. This study used ANSYS Workbench to compare two aluminum alloys: 6061-T6 and 7075-T6 across four load cases. Fig.9 and Fig.10 shows stress and deformation at combine loading condition. (3g+ Cornering+ Torque).

- **Static 1g:** Stress just over 20 MPa, deformation under 0.016 mm for both alloys. 6061-T6: FOS 13.60, safety factor 2.76. 7075-T6: FOS 25.11, safety factor 4.99. Both reached the full 10^7 cycle fatigue limit.
- **Static 3g:** Stress ~60.1 MPa, deformation ~0.046–0.048 mm. 6061-T6: FOS 4.59, safety factor 2.42. 7075-T6: FOS 8.37, safety factor 3.85. Both at full 10^7 cycles.
- **3g + Cornering + Torque:** Stress 79.348 MPa. 6061-T6: FOS 3.47 (lowest in this study), safety factor 1.83. 7075-T6: FOS 6.33, safety factor 2.92. Both at full 10^7 cycles.
- **Cornering + Braking:** Stress 67.109 MPa. 6061-T6: FOS 4.11, safety factor 2.17. 7075-T6: FOS 7.49, safety factor 3.45.

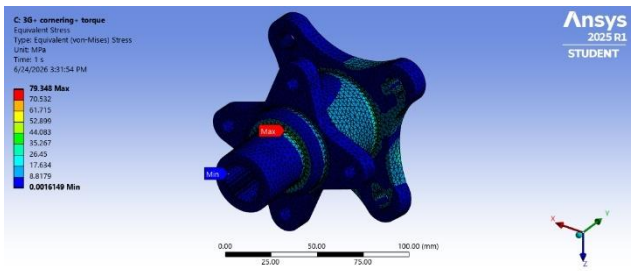

Fig.9 Stress at 3g+ Cornering+ Torque

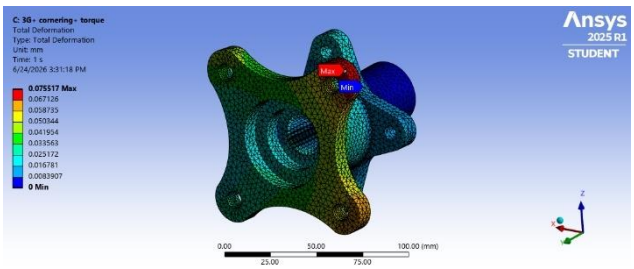

Fig.10 Deformation at 3g+ Cornering+ Torque

4.3 Knuckle Analysis

International Journal of Engineering Research & Technology (IJERT)
ISSN: 2278-0181
Vol. 15 Issue 06 , June - 2026

The knuckle connects the hub assembly to the suspension, transferring vertical, cornering, and braking loads. It was modeled using the same two aluminum alloys and four load cases as the hub.Fig.11 shows stress and Fig.12 shows deformation on knuckle.

- **Static 1g**: Stress 10.883 MPa for both alloys. 6061-T6: FOS 25.36, safety factor 13.63. 7075-T6: FOS 46.21, safety factor 15, the highest margins recorded anywhere in this study.
- **Static 3g:** Stress 32.662 MPa. 6061-T6: FOS 8.45, safety factor 4.4526. 7075-T6: FOS 15.4, safety factor 7.0832.
- **3g + Cornering + Torque:** Stress 36.525 MPa. 6061-T6: FOS 7.55 (lowest in this component's study), safety factor 3.9817. 7075-T6: FOS 13.77, safety factor 6.3341, both still well above 1.0.
- **Cornering + Braking**: Stress 44.483 MPa. 6061-T6: FOS 6.205, safety factor 3.2694. 7075-T6: FOS 11.3, safety factor 5.2009.

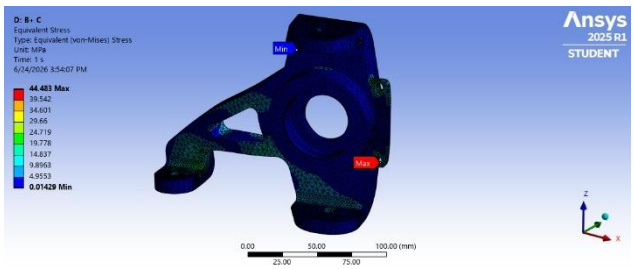

Fig.11 Stress at Cornering + Braking

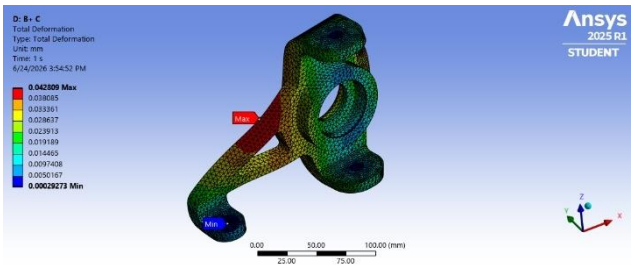

Fig.12 Deformation at Cornering + Braking

4.4 Chassis Analysis

The chassis ties the suspension, powertrain, and body into one structure and resists vertical, torsional, and impact loads. Three materials were compared: 6061-T6, Mild Steel, and AISI 4130 across four load cases. Fig.13 shows stress on chassis during torsional condition and Fig.14 shows deformation during on chassis at torsional test.

- **Static 1g**: Deformation 0.06459 mm (6061-T6, Mild Steel) and 0.063015 mm (AISI 4130); combined stress identical at 6.8498 MPa for all three. FOS: 38.98 (6061-T6), 36.55 (Mild Steel), 67.16 (AISI 4130).
- **Static 3g:** Deformation highest for 6061-T6 (0.58835 mm) versus 0.20165 mm and 0.19673 mm for Mild Steel and AISI 4130. FOS: 12.41, 11.59, and 21.32 respectively.
- **Torsional Test:** 6061-T6 deformed far more (10.541 mm) than Mild Steel (3.558 mm) and AISI 4130 (3.4712 mm). FOS: 4.21 (6061-T6), 3.944 (Mild Steel — tightest margin in the study), 7.25 (AISI 4130).
- **Side Impact:** Deformation 0.35896 mm (6061-T6) versus 0.12306 mm and 0.12006 mm (Mild Steel, AISI 4130). FOS: 6.103, 6.276, and 11.5493 respectively.

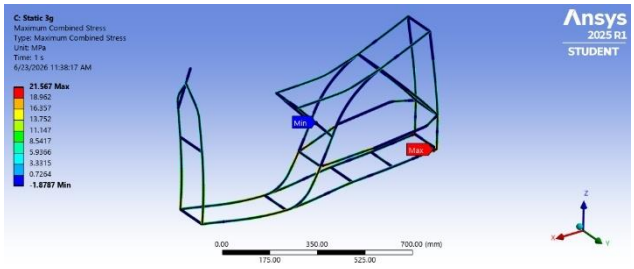

Fig.13 Stress at Torsional Test

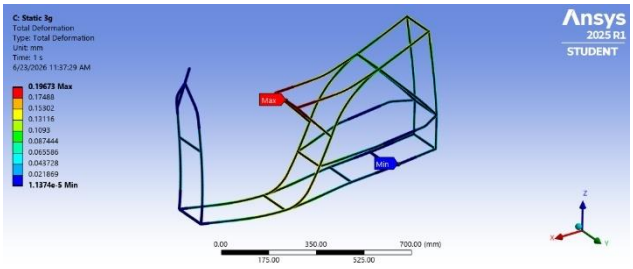

Fig.14 Deformation at Torsional Test

International Journal of Engineering Research & Technology (IJERT)
ISSN: 2278-0181
Vol. 15 Issue 06 , June - 2026

5 DISCUSSION

Across all four components, stress and deformation are governed mainly by load magnitude and geometry, while material choice determines the safety margin once that stress is known clearest in the chassis, where 6061-T6, Mild Steel, and AISI 4130 all produced nearly identical stress, with FOS separating only through yield strength.

A second pattern is the strength-versus-practicality trade-off. The hub and knuckle clear every load case comfortably with both 6061-T6 and 7075-T6, making cost and machinability the deciding factor 6061-T6 wins, since 7075-T6's extra strength goes unused. The wishbone and chassis tell a different story: Mild Steel's FOS drops below 1.0 in their most severe cases (3g bump, torsion), while AISI 4130 stays above 1.0 throughout, making the extra strength a structural necessity rather than a cost choice.

Fatigue results add nuance beyond static FOS. In the wishbone's 3g case, both materials show a fatigue safety factor below 1.0, yet Mild Steel fails at zero cycles while AISI 4130 survives over 16,000, showing fatigue life and safety factor are separate, complementary measures. Different fatigue targets were used for steel (10^7 cycles) and aluminum (10^6 cycles), reflecting steel's true endurance limit versus aluminum's lack of one.

Overall, components facing rare, severe loads (wishbone bump, chassis torsion) require a stronger material, while components facing steady, moderate loads (hub, knuckle) can use a cheaper one without compromising safety.

6 RESULT

The structural analysis of the wishbone, hub, knuckle, and chassis shows that stress and deformation depend mainly on load magnitude and geometry, while material choice mainly affects the safety margin available once that stress is known. Combined stress came out nearly identical across materials in the chassis results, for example, with the real difference showing up only in factor of safety.

The hub and knuckle results show that both 6061-T6 and 7075-T6 clear every load case comfortably, including the toughest combined condition. Since 6061-T6 already provides enough margin, the deciding factor becomes practical: it is cheaper and easier to machine and weld, while 7075-T6's extra strength goes largely unused. This shows that picking the strongest available material isn't always the most efficient choice. The wishbone and chassis tell a different story. Mild Steel's FOS drops below 1.0 in the wishbone's 3g case and the chassis torsional case — its two most severe conditions — while AISI 4130 avoids this in every case. Here, the extra strength isn't optional; it's a structural necessity.

Fatigue results add further nuance: in the wishbone's 3g case, both materials show a fatigue-based safety factor below 1.0, but their actual cycle counts differ by orders of magnitude (zero for Mild Steel versus over 16,000 for AISI 4130). This shows that a safety factor just under 1.0 doesn't always mean imminent failure — the real cycle count still matters. Different fatigue life targets were used for steel (10^7 cycles) and aluminum (10^6 cycles) since steel shows a true endurance limit while aluminum does not. Overall, the four components point to one general principle: where a component's worst-case load is rare and severe, like the wishbone's bump impact or the chassis torsional twist, a stronger material is justified. Where the load stays moderate and predictable, like the hub and knuckle, a lower-cost material can meet every requirement without compromise.

FUTURE SCOPE

- Build a physical prototype to validate the analytical and FEA results against real-world strain gauge measurements and on-road fatigue testing.
- Extend the suspension analysis using full multi-body dynamic simulation, incorporating tire and road input for a more complete ride and handling evaluation.
- Develop a detailed electrical system, covering motor controller selection, battery management system (BMS) design, and thermal management, to move from sizing-level calculations to a buildable powertrain.

REFERENCES

[1] William F. Milliken & Douglas L. Milliken, Race Car Vehicle Dynamics, Fundamentals of Vehicle Dynamics and Stability

[2] S. Patil et al. (2021), IJMET, Analysis of Suspension System for Light Electric Vehicle

[3] Thomas D. Gillespie, Fundamentals of Vehicle Dynamics. SAE International, 1992

International Journal of Engineering Research & Technology (IJERT)
ISSN: 2278-0181
Vol. 15 Issue 06 , June - 2026

[4] S. Shinde, P. Patil and A. Jadhav, "Design and Structural Analysis of Wheel Hub Using Finite Element Method," IRJET, 2018.

[5] Kunal Garde, Pranav Shinde, Rushikesh Jirage, “Design and optimization of hub and knuckle for Formula SAE car”, 2014/2015.

[6] Dusane et al. – Analysis of Steering Knuckle of All Terrain Vehicles Using Finite Element Analysis.

[7] Society of Indian Automobile Manufacturers (SIAM). Annual EV Sales Statistics 2025.

[8] NITI Aayog / Ministry of Heavy Industries. FAME Scheme and PM E-DRIVE Initiative — Policy Documents. Government of India.

[9] ANSYS Inc. ANSYS Workbench Mechanical User's Guide — Meshing Methods (Automatic, Patch Conforming Tetrahedron, Beam Elements). ANSYS Documentation.

[10] Bhandari, V.B. Design of Machine Elements. Tata McGraw Hill Education, New Delhi.

[11] Bairagi, K., et al. Kinematic Analysis and Structural Design of Suspension Wishbone for a Solar Electric Vehicle. International Journal of Vehicle Systems Modelling and Testing, 17(3/4), 288–310 (2023).

[12] Patil, V., Sawant, P., Shinde, S., Chavan, N., Pasare, V. Design and FEA Model of Double Wishbone Suspension for Student Formula Prototype Vehicle. D.Y. Patil College of Engineering and Technology, Kolhapur, 2022.

[13] Krishnan, P., et al. Static and Fatigue Simulation of Telescopic Fork Suspension System Used for Motorcycle. International Journal of Applied Engineering Research, 10(71), 2015.

[14] Design and Analysis of Suspension System for E-Bike. International Journal of Engineering Research and Development, 14(5).